

Structure Optimization Combining Soft-Core Interaction Functions, the Diffusion Equation Method, and Molecular Dynamics

Thomas Huber,[†] Andrew E. Torda,[‡] and Wilfred F. van Gunsteren^{*§}

Research School of Chemistry, Australian National University, Canberra, 0200 NSW, Australia, and
Physical Chemistry, ETH Zentrum, CH-8092 Zürich, Switzerland

Received: March 11, 1997; In Final Form: June 11, 1997[⊗]

Smoothing the potential energy surface for structure optimization is a general and commonly applied strategy. We propose a combination of soft-core potential energy functions and a variation of the diffusion equation method to smooth potential energy surfaces, which is applicable to complex systems such as protein structures. The performance of the method was demonstrated by comparison with simulated annealing using the refinement of the undecapeptide Cyclosporin A as a test case. Simulations were repeated many times using different initial conditions and structures since the methods are heuristic and results are only meaningful in a statistical sense.

Introduction

Most nonlocal optimization methods for molecular structures work by surmounting hurdles on the uneven potential energy landscape and moving along the overall gradient toward the global minimum. Probably the most popular approach is simulated annealing,¹ which reduces the size of barriers with respect to the kinetic energy of the system. Other methods would include potential energy annealing conformational search (PEACS),² which attempts to coax a system around bumps in the energy surface by coupling it to an external potential energy surface. One might attempt to smooth a surface by filling in the energy hypervalleys.^{3–5} Several other methods temporarily add artificial degrees of freedom,^{6–8} which can be seen as smoothing the energy surface with respect to the initial, physically real degrees of freedom. Some approaches are based on the smoothing of a mean field potential energy surface.^{9–16} The strategy is more obvious in methods that apply smoothing procedures directly, such as the deflation method¹⁷ and diffusion equation method (DEM).^{18–22} In the last method, the diffusion equation is solved analytically for potential energy surfaces and the original potential energy surface is restored by a time reversal process. This method has been successfully applied on difficult test problems in global optimization,²⁰ but is not easy to implement for general interaction functions used in structure refinement and performs less well in the field of structure optimization where steep slopes move the global minimum of the smoothed energy surface far away from the actual global minimum. In this case, only extremely slow restoration of the original surface can guarantee good results. To specifically address this problem, we have used a method where the extrema of different terms in the energy function are maintained and only their shape is modified during the smoothing process. Although this does not guarantee that the global minimum will be fixed during the smoothing process, it keeps it close to the original position and the reverse process can be performed more quickly. We have applied this approach to the modification of a conventional molecular dynamics force field.²³ As a test case, we have considered the refinement of an undecapeptide with respect to the potential energy and a set of experimental NMR restraints.²⁴ This problem is small enough to allow repeated

calculations but is sufficiently difficult to challenge current optimization methods. It is also sufficiently well studied to allow comparison with earlier work.^{2,5,8}

Theory

We wish to modify the potential energy surface such that an increase of a smoothing parameter t reduces the barriers separating minima and the system is able to cross them easily. Piela et al.¹⁸ introduced the idea of applying the second-order differential operator equation, which describes heat and diffusion processes to the potential energy function.

$$\frac{\partial^2}{\partial x^2} = \frac{\partial}{\partial t} \quad (1)$$

The solution of this operator equation when applied to a function depends on a new variable t , which controls the modification of the function. As seen directly from the differential equation, the function changes with a change of t depending on the local curvature. This has the effect that barriers “melt” and minima gradually “fill up” when t increases.

We followed this idea of modifying potential energy surfaces according to their local curvature, but in contrast, the diffusion operator was not applied to the total potential energy function. Instead, separate energy terms were smoothed independently. Improper dihedral angle, bond length, and bond angle changes are less important for overall conformational changes so these terms of the interaction function were not smoothed. On the other hand, contributions from dihedral angle and nonbonded interaction terms appeared to determine the probability of conformational transitions and therefore were replaced by smoothable functional forms. Piela et al.¹⁹ derived and summarized analytic solutions for different functional forms including Gaussian functions, which are most suitable for this purpose. The well-known solution when the operator equation (1) is applied to a Gaussian function of the form

$$f(x) = A \exp(-B(x - C)^2) \quad (2)$$

is

$$f(x;t) = \frac{A}{\sqrt{1 + 4Bt}} \exp\left(-\frac{B(x - C)^2}{1 + 4Bt}\right) \quad (3)$$

[†] Australian National University. Thomas.Huber@anu.edu.au.

[‡] Australian National University. Andrew.Torda@anu.edu.au.

[§] ETH Zentrum. wfvgn@igc.chem.ethz.ch. Fax: +41-1-632 1039.

[⊗] Abstract published in *Advance ACS Abstracts*, July 15, 1997.

Van der Waals Potential Energy Term. To make large local rearrangements possible, it is often useful to replace Lennard-Jones interaction functions by functions with finite values at zero distance. These interaction functions introduced by Levitt²⁵ are referred to as soft-core potential energy functions.^{26–28} Smoothing the energy hypersurface speeds up the system's convergence to the global energy minimum, since the size of barriers surrounding local minima is reduced and less time is spent in order to overcome these barriers. This led to the use of a switching function based on whether a distance was greater than the distance of minimum interaction energy, r_0 ,

$$V_{ij}^{\text{vdW}}(r) = \begin{cases} V_{ij}^{\text{soft}}(r) & r < r_0 \\ V_{ij}^{\text{Gauss}}(r) & r \geq r_0 \end{cases} \quad (4)$$

where

$$V_{ij}^{\text{Gauss}}(r) = V_{ij}^0 \exp(-B(r - r_0)^2) \quad (5)$$

with $B = 2r_0^{-2}$ describing the width of the function and V_{ij}^0 the potential energy at the distance of minimum energy in the original Lennard-Jones form. The soft-core interaction term of (4) was given by

$$V_{ij}^{\text{soft}}(r) = V_{ij}^0 + V_{\text{barrier}} \left(1 - 2\left(\frac{r}{r_0}\right)^2 + \left(\frac{r}{r_0}\right)^4 \right) \quad (6)$$

This function was chosen since it has a finite value, $V_{\text{barrier}} + V_{ij}^0$, even when two particles completely overlap ($r = 0$). Expressions (5) and (6) are chosen such that the total energy (4) is continuous and equal to V_{ij}^0 at $r = r_0$, has a continuous derivative equal to zero at $r = 0$ and $r = r_0$, and has a curvature equal to $-4V_{ij}^0 r_0^{-2}$ at $r = r_0$ (if r approaches r_0 from above).

During the smoothing process, the soft-core part of the interaction function changes with the smoothing variable t_{nb} according to

$$V_{ij}^{\text{soft}}(r; t_{\text{nb}}) = V_{ij}^{\text{soft}}(r) (1 + 4Bt_{\text{nb}})^{-1/2} \quad 0 \leq r \leq r_0 \text{ and } t_{\text{nb}} \geq 0 \quad (7)$$

and the Gaussian part of the interaction function according to

$$V_{ij}^{\text{Gauss}}(r; t_{\text{nb}}) = V_{ij}^0 \exp\left(-\frac{B(r - r_0)^2}{1 + 4Bt_{\text{nb}}}\right) (1 + 4Bt_{\text{nb}})^{-1/2} \quad r \geq r_0 \text{ and } t_{\text{nb}} \geq 0 \quad (8)$$

This choice implies that $V_{ij}^{\text{vdW}}(r; t_{\text{nb}})$ defined analogously to (4) is continuous at $r = r_0$ and has a derivative with respect to r that is equal to zero at $r = r_0$ for all $t_{\text{nb}} \geq 0$. Moreover, we have

$$V_{ij}^{\text{vdW}}(r; t_{\text{nb}}=0) = V_{ij}^{\text{vdW}}(r) \quad (9)$$

We note, however, that $V_{ij}^{\text{soft}}(r; t_{\text{nb}})$ does not satisfy the diffusion equation, whereas $V_{ij}^{\text{Gauss}}(r; t_{\text{nb}})$ does.

Electrostatic Potential Energy Term. To model electrostatic interactions, we followed the same principle. Coulombic interactions were approximated with three Gaussian functions of type (8) centered at the origin ($r = r_0$) using a least-squares fit in the range 0.3–1.2 nm, varying the three pairs of parameters V_{ij}^0 and B .

Dihedral Angle Potential Energy Term. Trigonometric functions of the form

$$V(\phi) = k_\phi (1 - \cos(n\phi - \delta)) \quad (10)$$

are often used to describe rotational barriers around a dihedral angle, where k_ϕ is a scaling factor, n is the periodicity, and δ is a phase shift.

Since the dihedral angle potential energy surface was deformed independently of other potential energy terms, the transformation of this potential energy function term could be done in dihedral angle space. It can easily be shown that

$$f(x; t) = \exp(-\omega^2 t) \cos(\omega x - \delta) \quad (11)$$

is a solution of the diffusion equation for the trigonometric function of the form

$$f(x) = \cos(\omega x - \delta)$$

Thus, the diffusive dihedral angle potential energy term is given by

$$V^{\text{dih}}(\phi; t_{\text{dih}}) = k_\phi (1 - \exp(-n^2 t_{\text{dih}}) \cos(n\phi - \delta)) \quad t_{\text{dih}} \geq 0 \quad (12)$$

We note that the location of the minima of each energy term is not disturbed by the smoothing process, i.e., is not dependent on t . Only the depth and local environment are changed. Figure 1 shows the effect of smoothing on a dihedral angle potential energy function. The smoothing processes for the dihedral angle term and nonbonded interactions are taken to be completely independent. This allows one to use different rates for deforming and restoring the energy contributions from each term.

Methods

All simulations concerned Cyclosporin A and were conducted in vacuo using a leap frog integration scheme with a time step of 2 fs. The SHAKE algorithm²⁹ was applied to constrain bond lengths. All nonbonded interactions were evaluated without truncation of forces beyond a cutoff radius. An extra term was included in the potential energy function to force the molecule to satisfy a set of 57 distance restraints, experimentally determined by NMR.²⁴ This term was harmonic with respect to distance restraint violations with a force constant of 4000 kJ mol⁻¹ nm⁻². Nine distinctly different conformations (class 1–9) that satisfy experimental restraints³⁰ were used as initial structures in the simulations. For each of the nine structures, ten calculations were performed with different initial velocity assignments.

Interaction parameters for the Gaussian-based functional form were obtained by a least-squares fit to GROMOS interaction functions with the GROMOS 37D4 vacuum force field parameters.²³ The fit was performed for distances in the range 0.3–0.9 nm for van der Waals interactions and in the range 0.3–1.2 nm for Coulomb interactions.

In simulated annealing simulations, the initial velocities were assigned according to a temperature of 1200 K, and within 100 ps simulation time, the temperature was lowered exponentially to 300 K. In calculations using the diffusion equation to smooth the energy surface, the atom velocities were assigned and kept to a temperature corresponding to 300 K. The simulation length was half the number of steps of the simulated annealing simulations, using approximately the same amount of CPU time. In both types of simulations, Berendsen's weak coupling method³¹ was used to control temperature. With the combination of diffusion equation-smoothing and soft-core potential energy terms, the temperature coupling constant τ_T was 0.02

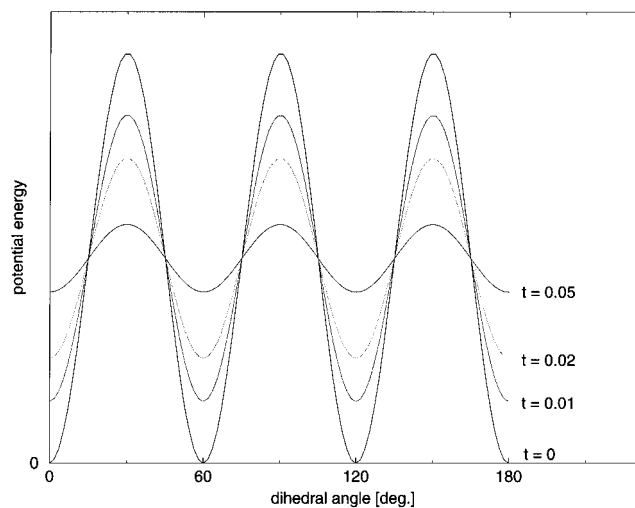


Figure 1. Smoothing of a dihedral angle term with the diffusion equation. Each curve shows $V^{\text{dih}}(\phi; t_{\text{dih}})$ for a different value of t_{dih} as labeled. The original potential energy is given by $t_{\text{dih}} = 0$. Parameter values are $n = 6$ and $\delta = 0$.

ps. In simulated annealing simulations, the system was coupled more tightly with τ_T equal to the integration time step.

In calculations using the diffusion equation and soft-core interaction functions, in the first 2500 steps the smoothing parameter t_{nb} was changed linearly from $t_{\text{nb}} = 0 \text{ nm}^2$ to its maximal value $t_{\text{nb}}^{\text{max}}$. To avoid another adjustable parameter in the simulations, the value of t_{dih} was set to $t_{\text{dih}} = 0.1 t_{\text{nb}}$. Then in the reverse process, t_{nb} and t_{dih} were exponentially lowered to $t_{\text{nb}} = 10^{-5} \text{ nm}^2$ and $t_{\text{dih}} = 10^{-6}$, respectively. All simulations were performed using the same soft-core barrier height $V_{\text{barrier}} = 50V_{ij}^0$.

All final structures were relaxed by a short MD simulation of 5 ps in the original GROMOS 37D4 force field. The SHAKE algorithm was not used to hold bond lengths constant. Subsequently, the potential energy was minimized with 10000 function evaluations in a quasi Newton minimization method or stopped when the total gradient was less than $10^{-6} \text{ kJ mol}^{-1}$ per step.

Results and Discussion

Figures 2 and 3 summarize the results from ten simulations for each of the nine starting structures using both simulated annealing and diffusive soft-core potential energy functions. Due to the heuristic nature of both search methods, overall performance can only be judged by performing numerous simulations starting from different conformations.

Figure 2 shows the initial and final energies for each starting class and compares the two approaches. Both optimization methods find structures of lower energy than the starting conformation, but in simulated annealing simulations results are quite predetermined by the starting conformation. In simulations with diffusive soft-core potential energy functions, conformations with energies close to the lowest energy are found starting from almost every structure. In many cases this requires crossing extremely high energetic barriers, which is, despite high temperatures, often impossible with simulated annealing. Therefore, final structures are quite similar to the starting structure (and thus to each other) when surrounding energy barriers are high. In fact, this is the case for most of our classes of starting conformations of Cyclosporin A.

The ability to cross conformational barriers or to lose memory of the starting conformation can be detected by comparing structures to some reference structure. We have used the starting conformation of class 9 as reference, as it is the lowest energy

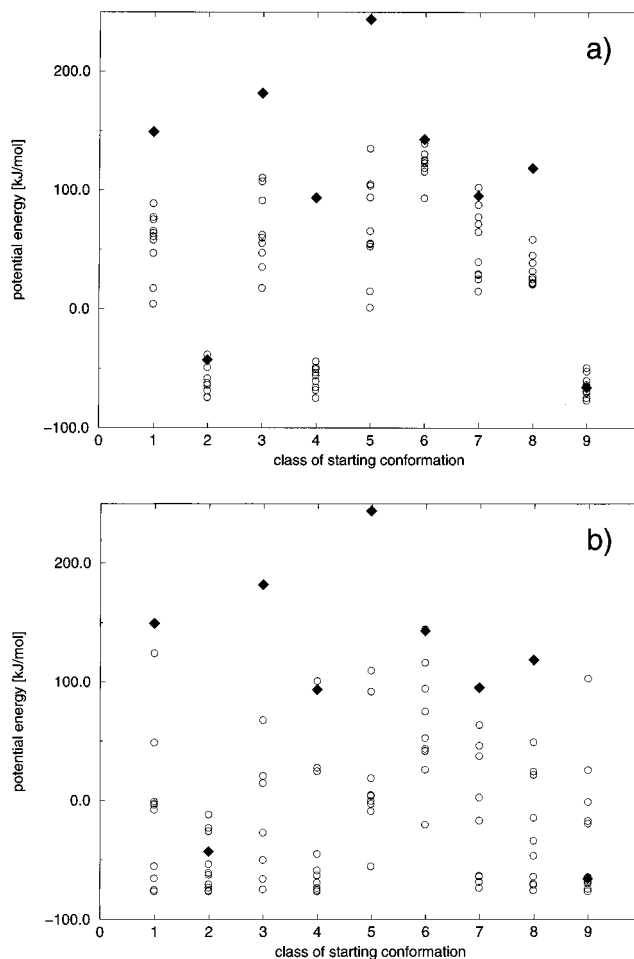


Figure 2. Energies of refined structures. The filled diamonds show the energies of the minimized starting structures: (a) simulated annealing; (b) diffusive soft-core potential energy functions, $t_{\text{nb}}^{\text{max}} = 1.0 \text{ nm}^2$. Each column shows results from a single starting structure. Open circles show the final energy of each calculation from the particular starting structure.

starting structure. Figure 3 shows the root mean square positional difference of all atoms for each final structure and this particular conformation. The small clusters of conformations in Figure 3a show the lack of ability to cross conformational barriers in the simulated annealing protocol used. Distinct clusters of points (e.g., class 6) indicate small conformational spread.

In contrast, calculations using a smoothed energy surface show a much greater conformational spread, even within classes (Figure 3c). This is due to the effect of making bigger parts of conformational space accessible when the potential energy surface is deformed. Unfortunately, simulation time is often not long enough to allow the system to settle down in low-energy regions. Energy barriers are built up again by reversal of the smoothing process and conformations may be trapped in areas of high potential energy. On the other hand, a bigger accessible space makes transition between low-energy conformations more likely. As a result, for each class of starting conformation, except when starting from class 6, in at least one out of ten diffusive soft-core potential simulations, low-energy conformations structurally close ($\text{RMSD} < 0.12 \text{ nm}$) to the class 9 conformation are found.

We tried to optimize the balance of making conformational space available and being able to find low-energy regions in this expanded space within a typical simulation time of 50 ps. Simulations were repeated for smoothing parameters $t_{\text{nb}}^{\text{max}} =$

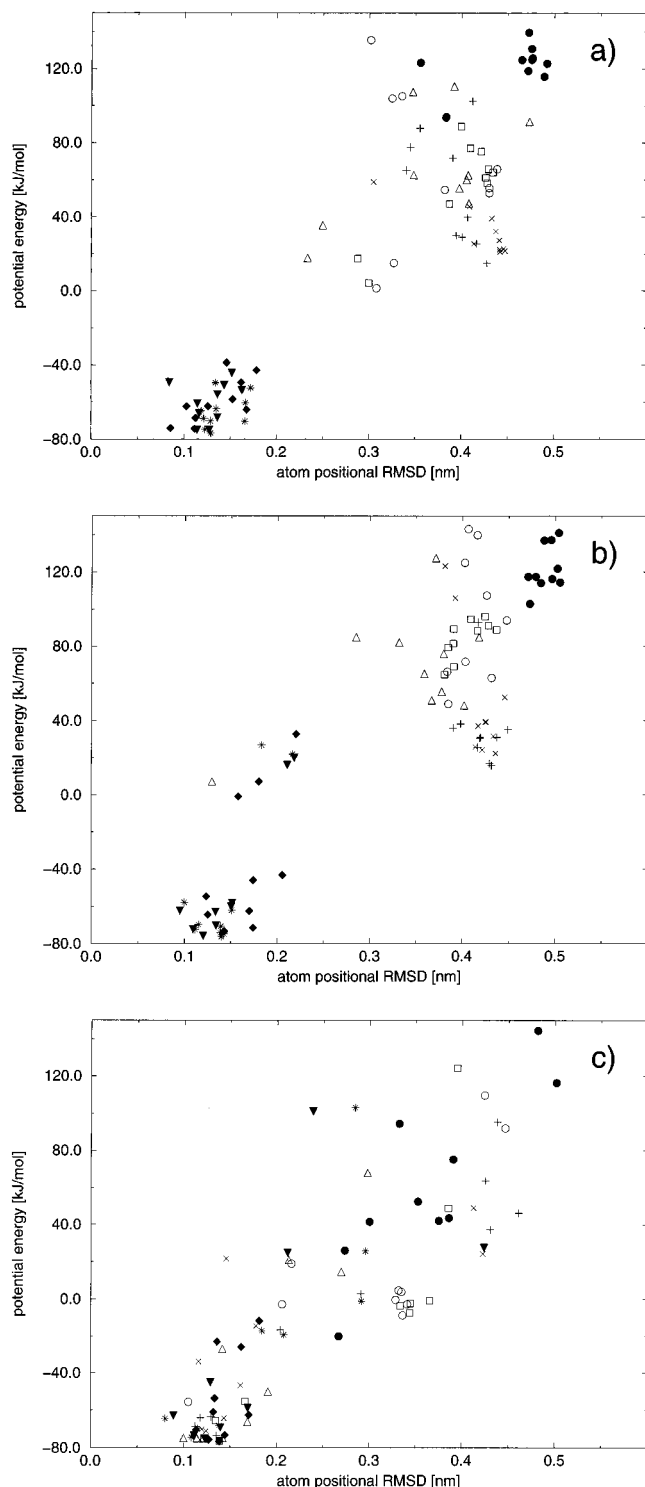


Figure 3. Comparison of the geometric spread of structures produced by the optimization methods: (a) simulated annealing results; (b) diffusion equation-smoothed soft-core potential energy method, $t_{nb}^{\max} = 0.1 \text{ nm}^2$; (c) diffusion equation-smoothed soft-core potential energy method, $t_{nb}^{\max} = 1.0 \text{ nm}^2$. Markers show the root mean square positional difference (RMSD) of all atoms in the final structure compared to the low-energy conformation, class 9. In both plots, members of the family of final structures for each starting conformation are shown using a common symbol, as labeled. Key: (\square) class 1; (\blacklozenge) class 2; (\triangle) class 3; (\blacktriangledown) class 4; (\circ) class 5; (\bullet) class 6; (+) class 7; (\times) class 8; (*) class 9.

0.1, 1, 2, 3, and 5 nm^2 . With $t_{nb}^{\max} = 0.1 \text{ nm}^2$, energetic barriers between low-energy conformations still seemed to be too high to be crossed (Figure 3b). A smoothing parameter of $t_{nb}^{\max} = 1 \text{ nm}^2$ was generally high enough to reduce energy barriers and

allow them to be overcome. Using smoothing parameters t_{nb} bigger than 2 nm^2 did not result in any further improvement.

Although we empirically optimized simulation parameters for the optimization protocols, there is no doubt that there is still room to improve results for each method. One could put forward the trivial argument that the temperature was not high enough in the annealing calculations and the spread of conformations could have been arbitrarily large. This of course would require a comparable increase in the cooling time. The intention here was to compare two methods using reasonable protocols and similar computational time. It genuinely appears that even with optimally tuned simulated annealing parameters the method would not perform as well as with dynamics simulations using diffusive soft-core potential energy functions. One reason is that high barriers, steep slopes, and narrow valleys are significant features of molecular potential energy surfaces. In this situation, simulated annealing often fails when the simulation time is limited. When the system is not sufficiently hot, the simulation time is often not long enough to allow barrier crossing. On the other hand, when the temperature is high enough to cross high energy barriers easily, the system is often unable to find the narrow valley of lowest energy within the cooling time.

Conclusions

The use of diffusive soft-core potential energy functions is a powerful method for molecular structure refinement with good overall performance and applicable to molecular systems without restrictions. Performance of optimization methods, however, is highly dependent on the optimization problem, and each method shows strengths and weaknesses.

This method's strength is the good performance in optimization problems with high energy barriers in which other optimization methods often fail. High energy barriers often involve steep slopes and narrow valleys, and since in this method the energy surface is deformed proportional to its local curvature, these parts of the potential energy function are affected most. This is especially important in the area of biomolecular modeling where huge energetic barriers often separate distantly close minima due to the dense packing of atoms.

A drawback of this approach is that, unlike the diffusion equation method, the deformed potential energy surface no longer has a single minimum for large values of the smoothing parameters. Therefore a combination with other heuristic search methods, such as molecular dynamics, is still useful. While the diffusive soft-core method is heuristic and does not guarantee good results in a single calculation, it displays good performance in comparison with other well-established heuristic methods such as simulated annealing.

Acknowledgment. Financial support from the Schweizerischen Nationalfonds (project 5003-034442) is gratefully acknowledged.

References and Notes

- (1) Kirkpatrick, S.; Gelatt, C., Jr.; Vecchi, M. *Science* **1983**, *220*, 671–680.
- (2) van Schaik, R.; van Gunsteren, W.; Berendsen, H. *J. Comput. Aided Mol. Design* **1992**, *6*, 97–112.
- (3) Glover, F. *ORSA J. Comput.* **1989**, *1*, 190–206.
- (4) Glover, F. *ORSA J. Comput.* **1989**, *2*, 4–31.
- (5) Huber, T.; Torda, A.; van Gunsteren, W. *J. Comput. Aided Mol. Design* **1994**, *8*, 695–708.
- (6) Crippen, G. *J. Comput. Chem.* **1982**, *3*, 471–476.
- (7) Purisima, E.; Scheraga, H. *Proc. Natl. Acad. Sci. U.S.A.* **1986**, *83*, 2782–2786.
- (8) van Schaik, R.; Berendsen, H.; Torda, A.; van Gunsteren, W. *J. Mol. Biol.* **1993**, *234*, 751–762.

- (9) Gerber, R.; Buch, V.; Ratner, M. *J. Chem. Phys.* **1982**, *77*, 3022–3030.
- (10) Straub, J.; Karplus, M. *J. Chem. Phys.* **1990**, *94*, 6737–6739.
- (11) Elber, R. *J. Chem. Phys.* **1990**, *93*, 4312–4321.
- (12) Olszewski, K.; Piela, L.; Scheraga, H. *J. Phys. Chem.* **1992**, *96*, 4672–4676.
- (13) Zheng, Q.; Rosenfeld, R.; Vajda, S.; DiLisi, C. *Protein Sci.* **1993**, *2*, 1242–1248.
- (14) Koehl, P.; Delaure, M. *J. Mol. Biol.* **1994**, *239*, 249–275.
- (15) Mierke, D.; Scheek, R.; Kessler, H. *Biopolymers* **1994**, *34*, 559–563.
- (16) Huber, T.; Torda, A.; van Gunsteren, W. *Biopolymers* **1996**, *39*, 103–114.
- (17) Crippen, G.; Scheraga, H. *Proc. Natl. Acad. Sci. U.S.A.* **1969**, *64*, 42–49.
- (18) Piela, L.; Kostrowicki, J.; Scheraga, H. *J. Phys. Chem.* **1989**, *93*, 3339–3346.
- (19) Kostrowicki, J.; Piela, L. *J. Opt. Theory* **1989**, *69*, 269–284.
- (20) Kostrowicki, J.; Piela, L.; Cherayil, B.; Scheraga, H. *J. Phys. Chem.* **1991**, *95*, 4113–4119.
- (21) Wawak, R.; Wimmer, M.; Scheraga, H. *J. Phys. Chem.* **1992**, *96*, 5138–5145.
- (22) Kostrowicki, J.; Scheraga, H. *J. Phys. Chem.* **1992**, *96*, 7442–7449.
- (23) van Gunsteren, W.; Berendsen, H. Groningen molecular simulation (GROMOS) library manual; Biomos: Groningen, The Netherlands, 1987.
- (24) Loosi, H.; Kessler, H.; Oschkinat, H.; Weber, H.; Petcher, T.; Widmer, A. *Helv. Chim. Acta* **1985**, *68*, 682–704.
- (25) Levitt, M. *J. Mol. Biol.* **1983**, *170*, 723–764.
- (26) Nilges, M.; Clore, G.; Gronenborn, A. *FEBS Lett.* **1988**, *239*, 129–136.
- (27) Beutler, T.; Mark, A.; van Schaik, R.; Gerber, P.; van Gunsteren, W. *Chem. Phys. Lett.* **1994**, *222*, 529–539.
- (28) van Schaik, R. Novel search algorithms for biomolecular structure refinement. Ph.D. thesis, Rijksuniversiteit Groningen, Groningen, The Netherlands, 1994.
- (29) Ryckaert, J.-P.; Ciccotti, G.; Berendsen, H. *J. Comput. Phys.* **1977**, *23*, 327–341.
- (30) Lautz, J.; Kessler, H.; Blaney, J.; Scheek, R.; van Gunsteren, W. *Int. J. Peptide Protein Res.* **1989**, *33*, 681–288.
- (31) Berendsen, H.; Postma, J.; van Gunsteren, W.; DiNola, A.; Haak, J. *J. Chem. Phys.* **1984**, *81*, 3684–3690.